THE ASTROPHYSICAL JOURNAL, 384:467–473, 1992 January 10

THE ORIGIN OF THE OPTICAL EMISSION LINES ASSOCIATED WITH EXTRAGALACTIC RADIO SOURCES

S. M. VIEGAS
Instituto Astronômico e Geofísico, USP, Av. Miguel Stefano, 4200, 04301-São Paulo, SP, Brazil and European Southern Observatory, Karl-Schwarzschild Strasse 2, D-8046, Garching bei München, Germany

AND

E. M. DE GOUVEIA DAL PINO[1]
Harvard-Smithsonian Center for Astrophysics, 60 Garden Street, Cambridge, MA 02138
Received 1990 December 13; accepted 1991 July 15

ABSTRACT

We investigate the observed extended emission-line regions (EELRs) associated with the jets and lobes of low-redshift extragalactic radio sources with moderate power (3C 227, 3C 277.3, 3C 305, Cen A [NGC 5128], NGC 7385, PKS 0349−27, PKS 2152−69, and Minkowski's Object).

Using hybrid models which take into account the coupled effect of both the photoionization by a non-thermal radiation and the thermal collisions due to shocks, we calculated the line intensity ratio diagrams that best fit the observations. We found that the main energy sources of the EELR are: (1) a power-law radiation, with a flux at 1 Ryd $F_H \simeq (10^8$–$10^{10})$ cm^{-2} s^{-1} eV^{-1} and a spectral index $\alpha = 2.2$–2.8 (equivalent to 1.2–1.8 for a flux given in units of ergs cm^{-2} s^{-1} eV^{-1}), which probably originates at the central region of the galaxy, and (2) shocks with velocities $v_0 \simeq 300$–1000 km s^{-1} and preshock densities $n_0 \simeq 5$–100 cm^{-3}, resulting from the interaction of the relativistic plasma flow with the ambient medium. In all cases investigated, a [N/O] underabundance by a factor 4 relative to the cosmic value is required in order to explain the observed [N II]/[O II] line ratios. The ability of radio jets to interact with the ambient medium and stimulate star formation has been suggested by a number of observational works and demonstrated by a number of authors. Considering both the estimated lifetimes of the radio sources and the stellar evolution time scales, the [N/O] underabundance could be explained by a burst of star formation where only the more massive stars ($M \geq 8\ M_\odot$) have already evolved.

Subject headings: galaxies: jets — line: formation — radio continuum: galaxies — stars: formation

1. INTRODUCTION

A series of detailed radio and optical observations made over the last decade have helped to better establish the characteristics of extended emission-line regions (EELRs) associated with radio sources in different types of galaxies (Miley 1983; van Breugel 1986; Tadhunter 1987; Baum et al. 1988; Tadhunter, Fosbury, & Quinn 1989a).

The general properties of the EELRs are reviewed and summarized in a number of recent works (cf. van Breugel 1986; Robinson et al. 1987; Baum & Heckman 1989a, b; Fosbury 1989; Tadhunter et al. 1989a). Among the main results, we point out the following:

1. There is statistical evidence of a spatial relationship between the very extended emission-line region and the radio source, and statistical tendency of alignment of the EELRs with the source axis;

2. Although in many cases the gas motions appear to be predominantly gravitational, there are many examples in which the gas shows clear signs of interaction with radio jets. In such cases, the EELRs are generally produced near the boundaries of radio jets or lobes, and, in these regions, the jet is generally deflected and decollimated, and shows a low radio polarization;

3. The origin of the EELRs is still unclear, and probably different mechanisms are occurring in different sources, such as: (1) accretion from an external source (through galaxy mergers or tidal interactions) may be a likely origin for the gas in galaxies which show high angular momentum, disk structures, and morphological features like shells, loops, and tails (cf. Tadhunter et al. 1989a); (2) for galaxies with hot X-ray halos, it is quite plausible that the EELR gas has condensed out of a cooling flow (cf. Robinson et al. 1987; Tadhunter et al. 1989a); (3) another possibility is that the interstellar gas clouds have been drifted into the path of the jet causing their heating and entrainment (cf. van Breugel 1986); (4) alternatively, cool clumps or condensations could be produced inside the jet itself by thermal instabilities (Gouveia Dal Pino & Opher 1989a, b, 1990, 1991).

The facts above point to a possible association of the EELRs with star formation. The compression of the condensed gas by shocks induced by the interaction of the expanding jet with the ambient gas could drive the clumps over the Jeans limit and trigger star formation (de Young 1981; van Breugel et al. 1986). A similar mechanism is also suggested by Rees (1989) and Begelman & Cioffi (1989) to explain the recently discovered alignment of optical/infrared continuum and radio structure in the high-redshift radio galaxies (Chambers, Miley, & van Breugel 1987; McCarthy et al. 1987).

As discussed by different authors (cf. Robinson et al. 1987; Baum & Heckman 1989b), the ionization of the EELRs could result from photoionization by the continuum radiation from the galactic nuclei, or by young stars, and/or by thermal collisions due to shocks. Statistical analysis of a sample of 43

[1] On leave of absence from the Instituto Astronômico e Geofísico da Universidade de São Paulo, Brazil.

EELRs, predominantly associated with powerful radio galaxies, has shown several interesting results on the relationships between these line-emitting regions and the radio sources (Baum & Heckman 1989a, b). One of them is the correlation between the number of ionizing photons required to ionize the EELRs and the number of nuclear ionizing photons, suggesting that the nuclear Lyman continuum of the host galaxy is the main energy source of the EELRs. However, the contribution from other mechanisms (shocks, young stars, cosmic rays) may also be important, at least in low-power radio galaxies.

As long as the main strong optical emission lines are concerned, photoionization models of the EELRs seem to favor the nuclear ionizing continuum, as the energy source of these regions, and to exclude the ionization by young stars (Robinson et al. 1987). Some unexplained features of the observed emission-line spectra, as for example, the larger-than-predicted He II/Hβ and [O III] $\lambda4363/\lambda5007 + \lambda4959$ line ratios (cf. Tadhunter et al. 1989a), suggest the presence of an additional ionization mechanism (Fosbury 1989; Morganti et al. 1991; Tadhunter et al. 1989b). A similar situation is found in the narrow emission-line region (NLR) of active galactic nuclei (AGNs). Detailed analysis of the observations, based on theoretical models which account for the coupled effect of photoionization, shocks, and relativistic electrons, has shown that these processes are operating at different degrees in the NLR (Viegas-Aldrovandi & Contini 1989a, b, hereafter VAC89a,b; Viegas-Aldrovandi & Gruenwald 1988, 1990, hereafter VAG88 and VAG90).

Our goal in this paper is to study the emission-line region associated with radio sources in order to determine the characteristics of the ionization mechanisms and the possible effect of star formation. Until the present, a detailed comparison of the observed emission-line ratios with theoretical models which take into account the coupled effect of photoionization and shocks has not been done. The theoretical model and the observational data are presented in § 2. The results are shown in § 3. The discussion and final remarks appear in § 4.

2. OBSERVATIONAL DATA AND THEORETICAL MODEL

The characteristics of the ionization mechanism(s) of the EELRs can be determined by the comparison between the observed line ratios and the theoretical ones obtained from the models.

2.1. *Observational Sample*

From the observational data available in the literature, we selected the following low-redshift ($z < 0.09$) objects: 3C 227 (Prieto, Fosbury, & di Seregho Alighieri 1991, in preparation), 3C 277.3 (van Breugel et al. 1985b), 3C 305 (Heckman et al. 1982), Minkowski's object (van Breugel et al. 1985a), Cen A (Phillips 1981; Morganti et al. 1991), NGC 7385 (Simkin, Bicknell, & Bosma 1984), PKS 0349−27 (Danziger et al. 1984), and PKS 2152−69 (Tadhunter et al. 1987). Most of these objects show more than one emission-line region associated with the radio source, and in some cases observational data from the nucleus is also available. These objects are a subset of the sample recently investigated by Tadhunter et al. (1989a) and were selected because the [O III], [O II], and [O I] lines are observed in addition to [N II] and [Ne III] lines, allowing for the analysis of both high- and low-ionization lines. In addition, they are weak to moderate-power radio galaxies ($L_R < 10^{43}$ ergs^{-1}). The line ratios considered are [O III] $\lambda5007 + \lambda4959$/[O II] $\lambda3727$, [O I] $\lambda6300 + \lambda6363$/[O II] $\lambda3727$, $R_{\rm O\,III}$ = [O III] $\lambda4363$/[O III] $\lambda5007 + \lambda4959$, [N II] $\lambda6584 + \lambda6548$/[O II] $\lambda3727$, [Ne III] $\lambda3869 + \lambda3968$/[O III] $\lambda5007 + \lambda4959$, and He II $\lambda4686$/[O III] $\lambda5007 + \lambda4959$. The choice of these line ratios will become clear later on. When only the brighter component of the doublet is observed, we multiply its intensity by the factor 1.3 (obtained from the radiative probability data) in order to obtain the doublet total flux. The objects and the respective emission-line regions are listed in Table 1 with the adopted line ratios plotted in the diagnostic diagrams, except for the recent data on the EELRs of 3C 227 (Prieto et al. 1991) and of Cen A (see Tables 3 and 4 of Morganti et al. 1991). All data are corrected for reddening using the observed Hα/Hβ and assuming case B recombination.

2.2. *Photoionization Models*

In order to justify our choice of line ratios and to point out the difficulties faced by the photoionization models, let us briefly discuss them before describing our composite models. Note that most of the conclusions presented here are also valid for the NLR of AGNs and have been deeply analyzed in previous papers (VAC89a, b; VAG88; VAG90).

A first problem with photoionization of the EELRs by the nuclear radiation is the deficit in the number of ionizing photons required to explain the observed luminosity of most of

TABLE 1

OBSERVATIONAL DATA

Object	EELR	Reference	[O III]/[O II]	[O I]/[O II]	[Ne III]/[O III]	[N II]/[O II]	$R_{\rm O\,III}$	He II/[O III]
3C 277.3	Jet	1	5.56	0.29	0.05	0.35	...	...
	Lobe	1	0.75	0.08	<0.33	0.08	...	...
3C 305	Lobe	2	0.56	0.04	0.19	0.42	...	...
Minkowski	Jet	3	0.85	<0.03	0.06	0.24	<0.05	<0.02
Cen A[a]	Knot X	4	1.41	0.41	0.17	1.40	...	<0.02
NGC 7385	NE source	5	1.08	0.33	...	0.13	...	...
PKS 0349−27	E source	6	1.69	0.30	0.16	0.27	...	...
	W source	6	2.30	0.13	0.10	0.31	...	0.027
	Jet	6	4.15	0.21	0.09	0.57	0.019	0.044
PKS 2152−69	NE source	7	5.39	0.11	0.070	0.74	0.019	0.045

[a] Data for the inner and outer filaments of Cen A are not listed (see Morganti et al. 1991).

REFERENCES.—(1) van Breugel et al. 1985b; (2) Heckman et al. 1982; (3) van Breugel et al. 1985a; (4) Phillips 1981; (5) Simkin et al. 1984; (6) Danziger et al. 1984; (7) Tadhunter et al. 1987.

the objects, suggesting that other energy sources could be relevant to the EELR ionization (Baum & Heckman 1989a; Fosbury 1989). Let us recall that LINERs present the same difficulty (VAG90). However, if the nuclear continuum radiation is anisotropic, the problem with the lack of ionizing photons in the EELRs can be suppressed. This view is based on observational evidences and leads to a unified scheme for different classes of AGNs (Fosbury 1989).

Even if the problem of ionizing photon is solved assuming anisotropy of the nuclear radiation, the photoionization models fail in providing a complete understanding of the emission-line intensities (Robinson et al. 1987; Tadhunter et al. 1989b). The theoretical values of He II/Hβ, $R_{O\,III}$ and Fe X/Hβ are generally too small compared to observed values, whereas [O I]/Hβ is too high. Similar discrepancies are found for a large sample of NLRs of AGNs (VAC89b; VAG88; VAG90).

For AGNs, the observed [O I]/Hβ line ratio decreases as He II/Hβ increases, indicating that the emitting region is matter-bounded (Viegas-Aldrovandi 1988). Concerning the EELRs, values of He II/Hβ up to 0.5 are observed (Morganti et al. 1991) and cannot be reproduced by standard radiation-bounded models using a power-law spectrum with spectral index equal to 1.5 (or 2.5 if we use the flux in units of $cm^{-2}\ s^{-1}\ eV^{-1}$ as in this paper). However, it is easy to verify that such a line ratio can be obtained if the optical depth at the Lyman limit, τ_0, is less than 3. In addition, such a low optical depth would lead to low [O I]/Hβ values, that is, of the order of 0.5 (Viegas-Aldrovandi 1988). Therefore, the good fitting of low-ionization lines and He II λ4686 obtained by Morganti et al. (1991) for the filaments of Cen A using photoionization models is due to a low optical depth (for models with high-ionization parameters), more than to a multicloud effect. Although matter-bounded models may improve the fit to some line ratios, they are of no help in explaining Fe X/Hβ and $R_{O\,III}$.

Since the evidences favor matter-bounded models, we must be careful in the choice of line ratios when plotting the diagnostic diagrams. The [O I] line flux is extremely sensitive to τ_0, while [O III] and He II lines are not affected. Therefore, the choice of [O I]/[O III] line ratio (Robinson et al. 1987) may be misleading when analyzing a large sample of data, lumping together matter-bounded and radiation-bounded objects. In order to prevent as much as possible the effects of τ_0, we have used in our diagnostic diagrams the [O III]/[O II] line ratio instead of [O I]/[O III]. Low-ionization lines, such as [O II] and [N II], are less affected by the τ_0 value, the effect being larger for high values of the ionization parameter (VAG88).

Finally, let us point out that radiation-bounded models corresponding to a blackbody ionizing radiation with temperature higher than 1.5×10^5 K could give a good fit to the observed He II/Hβ, but the calculated low-ionization lines tend to be too strong (Binette, Robinson, & Courvoiser 1988). In addition, it does not solve the problem of the high observed $R_{O\,III}$ or the Fe X line.

2.3. *Composite Models*

Hybrid models, which take into account the coupled effect of both photoionization by a continuum radiation and thermal collisions due to shocks, improve the fitting to the observed line ratios of the NLR of AGNs. In the EELRs, shocks are likely to be induced by the interaction of jets with the interstellar medium. Although they are probably unable to provide the total emission-line luminosity (Whittle 1989), they could help to better understand the observed emission lines. In the following, a description of the model used is given.

TABLE 2

MODELS

Model	F_H ($cm^{-2}\ s^{-1}\ eV^{-1}$)	α	n_0 (cm^{-3})	v_0 (km s^{-1})	B_0 (G)
Z	10^8–10^{10}	2.2	100	300–1000	10^{-5}
Y	10^8–10^{10}	2.8	100	300–1000	10^{-4}
S.....	0	...	5–100	300–1000	10^{-5}

The theoretical values were computed from a composite model using the code SUMA which has been recently updated (VAC89b). The input parameters are the ionizing radiation spectrum characterized by the flux at 1 Ryd, F_H (in units of $cm^{-2}\ s^{-1}\ eV^{-1}$), and by the spectral index α (in the case of a power-law spectrum), the preshock density n_0, the shock velocity v_0, and the chemical composition of the gas. The model adopts a plane-parallel symmetry, and the effect of the magnetic field is also taken into account in the fluid equations (see, e.g., Cox 1972). Two types of models can be built with photoionization and shocks acting (1) on the same edge of the EELRs, or (2) on opposite sides.

A grid of models was calculated by varying F_H, α, n_0 and v_0. All of them were of type (1), that is, with the ionizing radiation reaching the EELRs at the shocked edge. Actually, considering the line ratios discussed here, the results of the type (1) and type (2) models are similar (VAC89a). Thus, we used a type (1) model in order to save computer time. The range of values for both parameters F_H and α were estimated from the observed optical continuum spectra of the nuclei extrapolated to the ultraviolet range. The values for the magnetic field intensities B_0 were obtained from the assumption of equipartition of energy between the relativistic electrons and the magnetic field (cf. Burns, Owens, & Rudnick 1979; Burns, Feigelson, & Schreier 1983). As discussed in previous papers, the model can be radiation-dominated or shock-dominated (VAC89a), depending mainly on the values of F_H and v_0 considered.

From all of the models considered, we selected those giving the best fit to the observed emission-line ratios (models Z, Y, and S). Notice that the value $\alpha = 2.5$,[2] generally adopted in the photoionization models (cf. Robinson et al. 1987), is an intermediate value between those adopted in the present work ($\alpha = 2.2$–2.8). A flatter spectrum ($\alpha = 2.2$) produces a large intermediate emitting zone, increasing the intensity of the low-ionization emission lines. On the other hand, results obtained with a steeper ionizing spectrum ($\alpha = 2.8$) could mimic matter-bounded models, since the volume of the intermediate zone is smaller and the low-ionization lines are less intense. Models with $\alpha = 2.5$ give emission-line ratio values which are intermediate between those obtained with the two extreme α values assumed. In addition to the corresponding input parameters listed in Table 2, a cosmic abundance was considered (Allen 1973). However, as we show below, the theoretical [N II] emission-line intensity may be too strong. Thus, models called ZN and YN were obtained considering a nitrogen underabundance of a factor of 4. Models S (with $F_H = 0$) are those where shock is the only ionization source.

Ionization by young stars has also been invoked as a possible process in the EELRs (van Breugel 1986). Thus, theoretical results obtained for H II regions (Gruenwald & Viegas-Aldrovandi 1992) were also taken into account.

[2] The spectral index $\alpha = 2.5$ corresponds to a power-law flux given in units of $cm^{-2}\ s^{-1}\ eV^{-1}$. If the flux is given in units of ergs $cm^{-2}\ s^{-1}\ eV^{-1}$, the corresponding value of the spectral index is 1.5, as usually found in the literature.

3. DIAGNOSTIC DIAGRAMS

The comparison between observational data and theoretical results appears in Figures 1 and 2 (high-ionization lines), and 3 and 4 (low-ionization lines). For the sake of clarity, the results corresponding to a particular model are not shown in these figures. Only the theoretical zone corresponding to a given type of model listed in Table 2 is plotted. These zones are delimited by solid (models Z), dotted-dashed (models Y), and dashed (models S) lines. Models for H II regions ionized by an O4 star and with hydrogen density $10 \leq n_H \leq 10^3$ cm^{-3} correspond to the dotted line, which is labeled by log (n_H) (= 1, 2, and 3, respectively). The line ratios listed in Table 1, coming from different observations, are all represented by filled squares, except the Minkowski's object which is denoted by a filled trapeze. Data for 3C 227 (Prieto et al. 1991) are shown as stars (if the distance D from the nucleus is less than 50 Kpc) or filled circles (if D is higher than 50 Kpc). The other symbols correspond to the inner and outer filaments of Cen A observed by Morganti et al. (1991) and follow the same notation as the one used by these authors (see their Fig. 7).

Let us point out how F_H and v_0, which determine the relative importance of photoionization and shock, influence the theoretical results. In Figures 1, 3, and 4, for a given type of model (Z or Y) an increase of F_H tends to move to the right the point

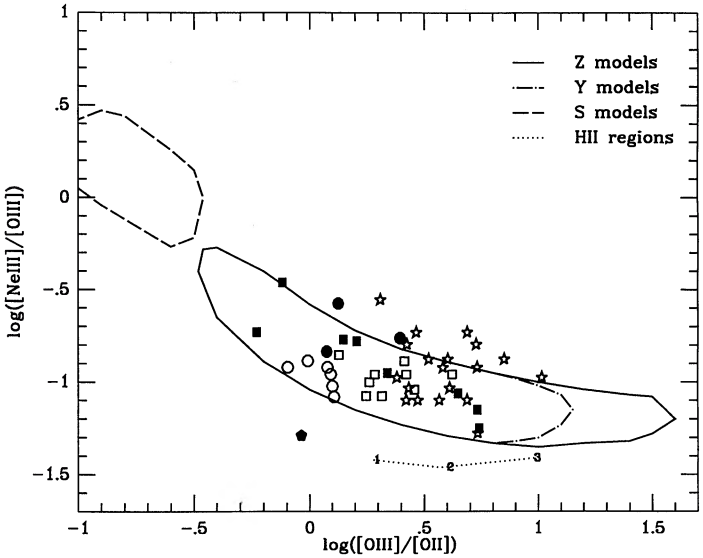

FIG. 1.—The [Ne III]/[O III] vs. [O III]/[O II] line ratios. Solid, dotted-dashed, and dashed lines indicate, respectively, the theoretical regions corresponding to models Z, Y, and S (see Table 2). Symbols correspond to the observed sample. The Cen A filaments (Morganti et al. 1991) are represented by different symbols according to their distance from the central source: slit-1 (*open circle*), slit-2 (*open square*), slit-3 (inner filament region) (*open triangle*), outer filaments (*filled triangle*). The 3C 277 data (Prieto et al. 1991) correspond to star symbols, if the distance from the nucleus is less than 50 Kpc, and to filled circles, if the distance is more than 50 Kpc. The EELR data listed in Table 1 are represented by filled squares, and the Minkowski's object is denoted by a filled trapeze.

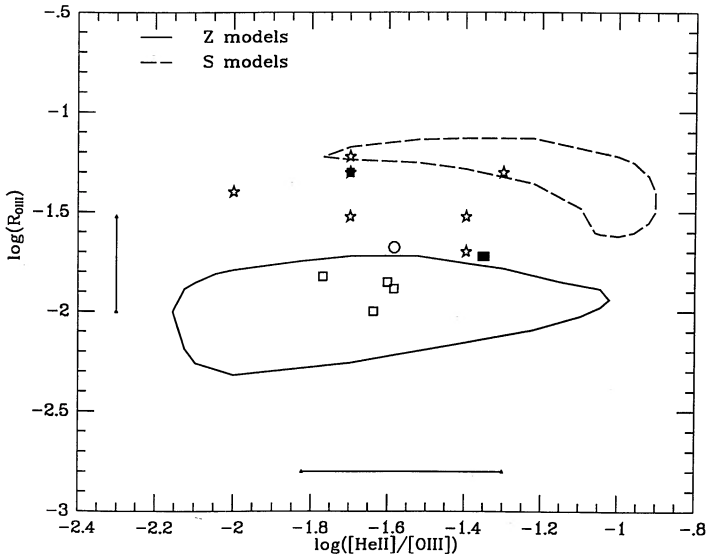

FIG. 2.—The $R_{O\,III}$ vs. He II/[O III] line ratios. Notation is the same as in Fig. 1. Theoretical regions defined by models Y and Z are practically coincident.

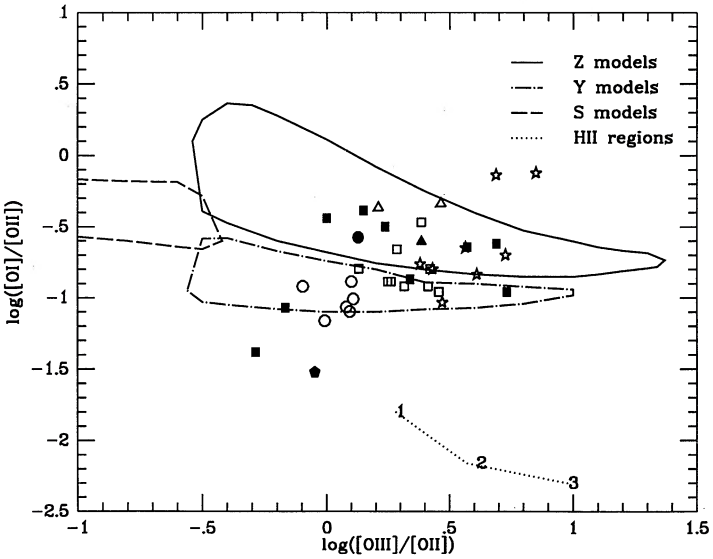

FIG. 3.—The [O I]/[O II] vs. [O II]/[O III] line ratios. Notation is the same as in Fig. 1.

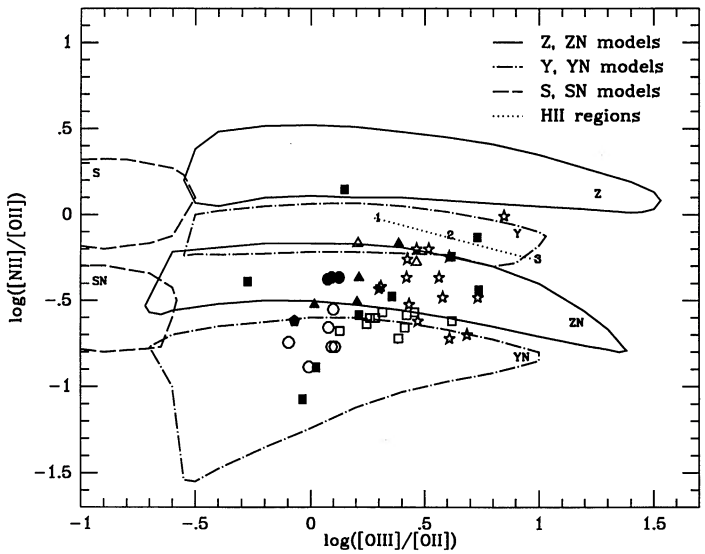

FIG. 4.—The [N II]/[O II] vs. [O III]/[O II] line ratios. Notation is the same as in Fig. 1. The theoretical regions corresponding to models YN and ZN (with the nitrogen abundance reduced by a factor 4) are also shown.

corresponding to the model, which is in agreement with the fact that the S zone ($F_H = 0$) is on the left of the other theoretical zones ($F_H \neq 0$). On the other hand, the theoretical point is shifted upward and to the left when v_0 increases. In Figure 2 a dominance of the shock effect over photoionization tends to move the corresponding point to the upper right part of the diagram.

There is an overlapping of the theoretical zones corresponding to the models Z and Y in Figure 1, which shows [Ne III]/[O III] versus [O III]/[O II] ratios. Except for the Minkowski's object, all the EELRs listed in Table 1 and showing [Ne III] lines can be fitted by these models, as well as the Cen A filaments. Notice that for the Minkowski's object the Hα/Hβ is uncertain by about 20% (van Breugel et al. 1985a), and a reddening correction higher than the adopted could move the corresponding ratios closer to the theoretical zone. The H II region models are not suitable.

The high-ionization line ratios that are not explained by the photoionization models are plotted in Figure 2, which shows $R_{O\,III}$ versus He II/[O III]. There are not many objects with both He II and [O III] λ4363 lines observed (only eight are available in the literature). Thus the vertical and horizontal bars indicate the range of the observed $R_{O\,III}$ and Hé II/[O III], respectively (Morganti et al. 1991; Tadhunter et al. 1989b), which includes objects other than those considered in this paper. The theoretical zones corresponding to models Y and Z practically coincide. Because these lines come from the high-ionization zone of the emitting region, the line ratios are mainly determined by the shock velocity. In addition, the effect of the photoionization is to increase the region where the temperature is of about 10^4 K, favoring the emission of [O III] nebular lines over [O III] λ4363, decreasing the $R_{O\,III}$ ratio. Therefore, for a given value of F_H, as the shock velocity increases from 300 to 1000 km s^{-1}, shock effects tend to dominate and the $R_{O\,III}$ ratio increases. It can be seen in the figure that the theoretical zone of the model S (shock only) corresponds to higher $R_{O\,III}$ than those given by models Y and Z, while the He II/[O III] ratios are similar.

In Figure 3, which shows [O I]/[O II] versus [O III]/[O II], the theoretical zones are practically disconnected. The EELRs of 3C 305 and Minkowski's object show an [O I]/[O II] line ratio too low to be fitted by the models. These objects seem to require matter-bounded composite models, even when the shock velocity is high and shock effects dominate radiation effects. In fact, high shock velocity models lead to a high-temperature postshock zone which produces diffuse radiation responsible for the increase of the emitting volume of the low-ionization region. Most of the Cen A filaments are in the theoretical zone defined by the models Y, although some of the parts of the inner filament (represented by open squares and open triangles) and the outer filament region (filled triangle) fall in the theoretical zone of the Z models. As in the previous diagrams, H II region models cannot reproduce the observed line ratios. In fact, such models give a weak [O I] line, but the line ratios do not correspond to the observed ones.

Figure 4 shows [N II]/[O II] versus [O III]/[O II]. Since most of the EELRs have [N II]/[O II] $\leq$ 0.6, models with cosmic [N/O] abundance ratios do not provide a good fit to the observations. The problem of high theoretical values of [N II]/[O II] could be related to the atomic data, to the optical depth, or to the [N/O] abundance ratio itself. Concerning the atomic data, they affect both the line emissivity (collision strength and radiative transition probability) and the ionization balance (photoionization and collisional ionizations, radiative and dielectronic recombinations, and charge transfer reactions). For the light elements ($A \leq 12$) the atomic data for the different processes are available in the literature and seem to be trustworthy. In fact, updated photoionization models provide a good fit to the emission-line spectrum of well-observed H II regions and planetary nebulae, and supply a good test to the atomic data. In addition, the NLR of AGNs show [N II]/[O II] ratios higher than 1, as obtained by updated standard photoionization models (VAG88). Thus, it seems unlikely that the disagreement between the observed and calculated [N II]/[O II] line ratios in the EELRs is due to uncertainties in the atomic processes. On the other hand, matter-bounded photoionization models could provide a smaller ratio, decreasing the theoretical value up to 0.25 for $U = 10^{-2}$. However, concerning the EELRs, the ionization parameter seems to be lower ($U \leq 5 \times 10^{-3}$), and the theoretical ratio is too high even considering matter-bounded models. Nevertheless, one could argue that objects with $0.1 <$ [N II]/[O II] < 0.8 should correspond to models Y or Z which are matter-bounded, with no nitrogen underabundance. Such models should move down the theoretical zones by up to a factor of 4 to match the observational data. However, the [O I]/[O II] theoretical ratio, being far more sensitive to opacity effects, would decrease by a higher factor (>8), leading to values too low compared to observations (see Fig 3). Finally, we see that models ZN and YN, with nitrogen underabundant by a factor of 4, give the appropriate [N II]/[O II] line ratio. A change in the nitrogen abundance tend to affect only the nitrogen emission-line intensities. In fact, since nitrogen is not a main coolant of the emitting gas, the physical conditions of the EELRs remain the same, and the emission lines of the other elements are not affected. The effect of changing the nitrogen abundance on models S is the same, that is, the theoretical region moves down. From all these considerations, we conclude that for most of the EELRs the observed [N II]/[O II] ratios can only be explained by an underabundance of N relative to O.

Finally, only one object in our sample (PKS 2152−69) show [Fe VII] and [Fe V] emission lines (Tadhunter et al. 1987). The observed intensities, relative to Hβ, are in the range of those observed in the narrow-line region of AGNs, which cannot be matched by photoionization models and could be a signature of shocks with velocities higher than 200 km s^{-1} (see Fig. 6 in VAC89a). The detection of these emission lines in other EELRs would also argue in favor of the presence of shocks in these regions and would strengthen the conclusions presented in this paper.

4. DISCUSSION AND CONCLUSIONS

As we show in Figures 1–4, the emission-line ratios of the EELRs considered in our sample can be explained by models which account for the coupled effect of photoionization and shock acting at different degrees. In addition, the figures show that the EELR ionization is not due to young stars. Robinson et al. (1987) reached the same conclusion. In fact, models for H II regions tend to give a [O I]/[O II] ratio too low, [O III]/[O II], $R_{O\,III}$ generally too high, and the He II line too weak. Minkowski's object shows features of starburst galaxies (van Breugel et al. 1985a), but standard models of H II regions cannot explain their observed line ratios. It is quite possible that giant H II regions are more complicated than a simple spherical nebula ionized by a central star. However, in this

object, the radio source associated with the optical emission-line region could also be contributing to the energy balance of the emitting gas, probably through shocks which modify the line spectrum. Considering all the EELRs analyzed here, our first conclusion is that the energy source of emission-line regions associated with radio sources is mainly due to a power-law radiation, probably originating in the central region of the galaxy, and to shocks resulting from the interaction of plasma flow, responsible for the radio emission, and the ambient medium.

It has been shown that the coupled effect of photoionization and shocks improves the fitting of the observed line ratios of the NLR, reproducing the spread of values in the diagnostic diagrams, and can be tested by line profile observations and X-ray observations (VAC89a,b; Contini & Viegas 1990). Similar tests apply to the EELRs.

The relation between the Hβ luminosity produced by shock and by photoionization has been previously analyzed (see Figs. 1 and 2 in VAC89a). With the input parameters used in our models (Table 2), it can be seen that models with $F_{\rm H} = 10^8$ cm^{-2} s^{-1} eV^{-1} are dominated by shock effects, even for low shock velocities. For models with higher $F_{\rm H}$ values and low shock velocities (≤ 500 km s^{-1}) the Hβ emission due to photoionization is of the order of, or smaller than, that produced by shock effect. For higher velocities, the shock contribution to Hβ is at least a factor of 2 higher than the photoionization one. Assuming that the shock velocity is similar to the [O III] component velocity, Whittle (1989) concludes that shocks are unlikely to be the only source of the emitting gas. Our analysis showed that shocks are necessary to explain the observed line ratios. Thus, in order to have a balance between photoionization and shock effects in the EELRs, we should expect that higher shock velocities would be associated with EELR reached by more intense ionizing fluxes, mainly if the emitting regions show high $R_{\rm O\,III}$ values. The results can be tested when observations of emission-line profiles for a large sample of EELRs become available.

The X-ray emission calculated by Contini & Viegas (1990), which could explain Seyfert 2 observations, corresponds to models with preshock densities higher than those considered in this paper. However, even with lower densities, high-velocity shocks (greater than 500 km s^{-1}) would produce X-rays in the high-temperature postshock region, which could be detected. For a preshock density of 10 cm^{-3}, and shock velocities between 600 and 1000 km s^{-1}, the postshock region would emit a soft (0.5–5 keV) X-ray flux in the range of 0.02–0.3 ergs cm^{-2} s^{-1}. Considering the size of one of the optical structures observed in Cen A, we would expect an X-ray luminosity of about 3×10^{39} ergs s^{-1}. Lower shock velocities would lead to lower luminosities: the luminosity is one order of magnitude lower for 500 km s^{-1}, and three orders of magnitude lower for 200 km s^{-1}. X-ray knots were observed in Cen A (Feigelson et al. 1981) with luminosities ranging from 5×10^{38} to 2×10^{39} ergs s^{-1} (assuming a distance of 5 Mpc). Thus, the shock effect invoked to explain the emission-line features could also account for the X-ray observations.

Another important issue is the [N/O] underabundance derived from our models. It is required to explain the observed [N II]/[O II] line ratios for most of the EELRs considered in this paper, which are at different distances from the nucleus of the host galaxy. One possible explanation is that the emitting gas corresponds to metal-poor halo gas. However, due to the optical depth effect on emitting gas, it would be difficult to determine the abundances relative to hydrogen required to confirm this hypothesis. In addition, notice that the points corresponding to the outer filaments of Cen A tend to have [N II]/[O II] higher than the inner filaments, which may indicate a higher [N/O] abundance farther away from the galactic nucleus. Another possibility is that local star formation is changing the [N/O] abundance ratio. Evidence of star formation have been found in the EELRs of high-redshift objects. In a smaller scale, the same phenomenon could occur in the EELRs of low-redshift galaxies studied in this paper. The estimated lifetime of the radio sources is $10^7 \leq t_R \leq 10^8$ yr (Miley 1980; Begelman, Blandford, & Rees 1984; Pelletier & Roland 1986; Begelman & Cioffi 1989). From stellar evolution models (Maeder & Meynet 1988), the evolution time for stars with mass $M \geq 8\ M_\odot$, which enrich the interstellar gas in oxygen and neon (Wheeler, Sneden, & Truran 1989), is $t_e \leq 5 \times 10^7$ yr, while stars with $M \leq 5\ M_\odot$, which produces nitrogen and carbon, have $t_e \geq 10^8$ yr. Thus, if stars are formed in the cooling gas associated with the EELRs, the more massive ones have enough time to evolve and enrich the emitting gas with oxygen and neon during the radio source lifetime and leading to a temporary [N/O] underabundance.

In our sample, the Minkowski's object shows evidence of star formation, and the observed [N II]/[O II] line ratio indicates an underabundance of N relative to O. Less convincing evidence is presented by three other objects: (1) the knot of NGC 7385 is bluer than its nucleus (Simkin et al. 1984), which could be attributed to star formation in the knot; (2) the 3C 305 spectrum shows absorption lines and a blue continuum that are not typical of an early-type galaxy and could be produced by young stars (Heckman et al. 1982); (3) some emission filaments of Cen A seem to be associated with blue objects (cf. Fosbury 1987; Graham & Price 1981). The other EELRs of our sample do not present evidence for star formation regarding the continuum emission or absorption lines. Since the EELRs have low surface brightness, deeper imaging is required to detect the continuum emission. In the future, star formation in the low-redshift EELRs could be tested by deep blue imaging, that should show the presence of massive young stars, by near-infrared observations of the Ca II triplet, which could reveal the presence of late-type stars (Terlevich, Diáz, & Terlevich 1990), and by ultraviolet observations of carbon lines, which should confirm a [C/O] underabundance.

We are deeply indebted to A. Prieto, R. A. E. Fosbury, and S. di Seregho Alighieri for making available their data in advance of publication, and to A. Prieto for many helpful discussions. We are thankful to J. Truran for stimulating conversations with one of us (S. M. V.) at the Aspen Center for Physics, and also to R. Opher for many suggestions and helpful comments, particularly at the beginning of this work. E. M. G. D. P. is also thankful to G. B. Field (NASA grant NAGW-931) and the other colleagues of the Harvard-Smithsonian Center for Astrophysics for their kind hospitality. Finally we would like to thank an anonymous referee whose helpful comments and suggestions have greatly contributed to improving this paper.

REFERENCES

Allen, C. W. 1973, Astrophysical Quantities (London: Athlone)
Baum, C. W., & Heckman, T. 1989a, ApJ, 336, 681
———. 1989b, ApJ, 336, 702
Baum, C. W., Heckman, T. M., Bridle, A. H., van Breugel, W., & Miley, G. K. 1988, ApJS, 68, 643
Begelman, M. C., Blandford, R. D., & Rees, M. J. 1984, Rev. Mod. Phys., 56, 255
Belgelman, M. C., & Cioffi, D. F. 1989, ApJ, 345, L21
Binette, L., Robinson, A., & Courvoisier, T. J. L. 1988, ApJ, 194, 65
Burns, J. O., Feigelson, E. B., & Schreier, E. J. 1983, ApJ, 273, 128
Burns, J. O., Owen, F. N., & Rudnick, L. 1979, ApJ, 84, 1683
Chambers, K. C., Miley, G. K., & van Breugel, W. 1987, Nature, 329, 604
Contini, M., & Viegas, S. M. 1990, ApJ, 350, 125
Cox, D. P. 1972, ApJ, 178, 143
Danziger, I. J., Fosbury, R. A. E., Goss, W. M., Bland, J., & Boksenberg, A. 1984, MNRAS, 208, 589
De Young, D. S. 1981, Nature, 293, 43
Feigelson, E. D., Schreier, E. J., Delvaille, J. P., Giacconi, R., Grindlay, J. E., & Lightman, A. P. 1981, ApJ, 251, 31
Fosbury, R. A. E. 1987, in Proc. 10th European Regional Meeting of the IAU (Prague: Astronomical Institute of the Czechoslovak Academy of Sciences), 351
———. 1989, Proc. ESO Workshop on Extragalactic Activity in Galaxies, ed. R. A. E. Fosbury & E. A. J. Meurs (Garching: ESO), 169
Gouveia Dal Pino, E. M., & Opher, R. 1989a, ApJ, 342, 686
———. 1989b, MNRAS, 240, 537
———. 1990, A&A, 231, 571
———. 1991, A&A, 242, 319
Graham, J. A., & Price, R. M. 1981, ApJ, 247, 813
Gruenwald, R. B., & Viegas-Aldrovandi, S. M. 1992, ApJS, 78
Heckman, T. M., Miley, G. K., Balick, B., van Breugel, W. J. M., & Butcher, H. R. 1982, ApJ, 262, 529
Maeder, A., & Meynet, G. 1988, A&AS, 76, 411
McCarthy, P. J., van Breugel, W., Spinrad, H., & Djorgovski, S. 1987, ApJ, 321, L29
Miley, G. K. 1980, ARA&A, 18, 165
———. 1983, in Proc. Conf. on Astrophysical Jets, ed. A. Ferrari & A. G. Pacholczyk (Dordrecht: Reidel), 99
Miley, G. K., & Chambers, K. C. 1989, in ESO Workshop on Extragalactic Activity in Galaxies, ed. J. A. Meurs & R. A. E. Fosbury (Garching: ESO), 43
Morganti, R., Robinson, A., Fosbury, R. A. E., di Serego Alighieri, S., Tadhunter, C. N., & Malin, D. F. 1991, MNRAS, 249, 91
Pelletier, G., & Roland, I. 1986, A&A, 163, 9
Phillips, M. M. 1981, MNRAS, 197, 659
Prieto, A., Fosbury, R. A. E., & di Seregho Alighieri, S. 1991, in preparation
Rees, M. J. 1989, MNRAS, 239, 1P
Robinson, A., Binete, L., Fosbury, R. A. E., & Tadhunter, C. N. 1987, MNRAS, 227, 97
Simkin, S. M., Bicknel, G. V., & Bosma, A. 1984, ApJ, 277, 513
Tadhunter, C. N. 1987, D.Phil. thesis, Univ. Sussex
Tadhunter, C. N., Fosbury, R. A. E., Binette, L., Danziger, I. J., & Robinson, A. 1987, Nature, 325, 504
Tadhunter, C. N., Fosbury, R. A. E., & Quinn, P. J. 1989a, MNRAS, 240, 225
Tadhunter, C. N., Robinson, A., & Morganti, R. 1989b, Proc. ESO Workshop on Extragalactic Activity in Galaxies, ed. R. A. E. Fosbury & E. A. J. Meurs (Garching: ESO), 293
Terlevich, E., Díaz, A. I., & Terlevich, R. 1990, MNRAS, 242, 271
van Breugel, W. J. M. 1986, Proc. Conf. on Jets from Stars and Galaxies, ed. R. N. Henriksen, Canadian J. Phys., 64, 392
van Breugel, W. J. M., Filippenko, A. V., Heckman, T. M., & Miley, G. 1985a, ApJ, 293, 83
van Breugel, W. J. M., Heckman, T., Miley, G. K., & Filippenko, A. V. 1986, ApJ, 311, 58
van Breugel, W. J. M., Miley, G. K., Heckman, T. M., Butcher, H. R., & Bridle, A. 1985b, ApJ, 290, 496
Viegas-Aldrovandi, S. M. 1988, ApJ, 330, L9
Viegas-Aldrovandi, S. M., & Contini, M. 1989a, ApJ, 339, 689 (VAC89a)
———. 1989b, A&A, 215, 253 (VAC896)
Viegas-Aldrovandi, S. M., & Gruenwald, R. B. 1988, ApJ, 324, 683 (VAG88)
———. 1990, ApJ, 360, 474 (VAG90)
Wheeler, J. C., Sneden, C., & Truran, J. W. 1989, ARA&A, 27, 279
Whittle, M. 1989, Proc. ESO Workshop on Extragalactic Activity in Galaxies, ed. R. A. E. Fosbury & E. A. J. Meurs (Garching: ESO), 199